IEEE Photonics Journal
An IEEE Photonics Society Publication

Open Access

Tuning of Plasmonic Resonances in the Near Infrared Spectrum Using a Double Coaxial Aperture Array

Volume 10, Number 6, December 2018

Miao Sun
Omid Kavehei
Paul Beckett
Ann Robert
William Shieh
Ranjith Rajeskharan Unnithan

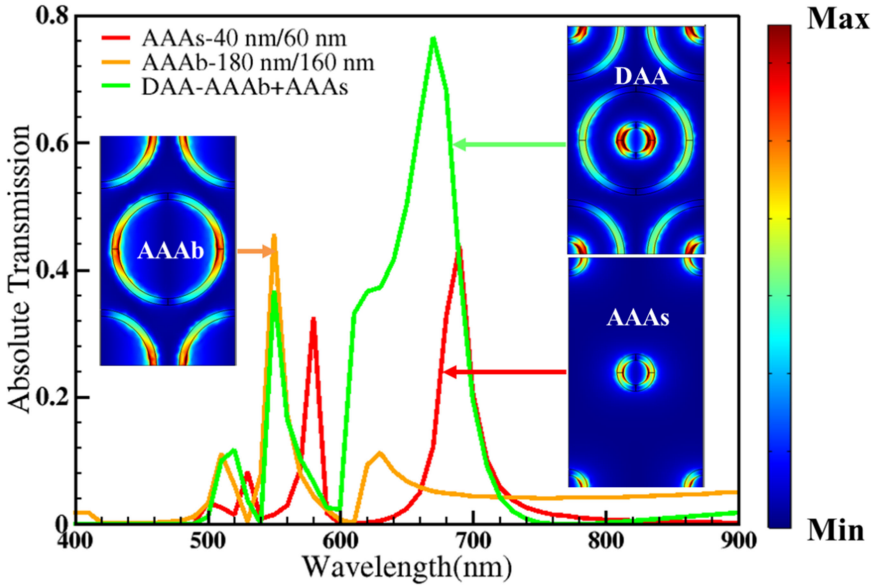

DOI: 10.1109/JPHOT.2018.2876898

Tuning of Plasmonic Resonances in the Near Infrared Spectrum Using a Double Coaxial Aperture Array

Miao Sun,[1] **Omid Kavehei**,[2] **Paul Beckett**,[3] **Ann Robert**,[4] **William Shieh**,[1] **and Ranjith Rajeskharan Unnithan** [1]

[1]Department of Electrical and Electronic Engineering, University of Melbourne, Melbourne, VIC 3010, Australia
[2]School of Electrical and Information Engineering, University of Sydney, Sydney, NSW 2006, Australia
[3]School of Engineering, RMIT University, Melbourne, VIC 3000, Australia
[4]School of Physics, University of Melbourne, Melbourne, VIC 3010, Australia

DOI:10.1109/JPHOT.2018.2876898

Manuscript received September 17, 2018; revised October 14, 2018; accepted October 15, 2018. Date of publication October 19, 2018; date of current version November 2, 2018. The work of R. R. Unnithan was supported by ARC through DP170100363. Corresponding author: Miao Sun (e-mail: miaos1@student.unimelb.edu.au).

Abstract: Plasmonic filters are excellent candidates for spectral filters in the near infrared spectrum. Such filters require only a single nanoscale thickness perforated metal film that can be tailored to tune the location of the transmission maximum. Here, we demonstrate using computational methods a double coaxial aperture array (DAA) in a hexagonal geometry that can be tuned to produce plasmon resonances accompanied by strong transmission in the near-infrared spectrum and at telecommunication wavelengths with a peak wavelength insensitive to angle of incidence. The DAA consists of two concentric annular apertures and radial distance between the two apertures is varied to tune the resonant wavelength. The presented geometry finds potential applications in modulators for telecommunication, spectroscopy, solar cells, high-resolution CMOS image sensors, chemical sensors, and biosensors.

Index Terms: Plasmonics, nanophotonics, subwavelength structures, photonic filters.

1. Introduction

Spectral filters are devices that can either transmit or reflect wavelengths of interest in the electromagnetic spectrum. Filters find applications in telecommunications, image sensors, medical devices, biosensors, new microscopes, light modulators and displays [1], [2]. Filter performance is evaluated using transmittance (T), reflectance (R), absorbance (A), and optical density. Current filter technologies are based on single cavity designs, pigments and dyes, multilayer coatings and Fabry-Pérot etalons [3], [4] in the visible, near infra-red (NIR) and far infra-red region. Frequency-selective bandpass and other filters have also attracted considerable interest for use in longer wavelength regions [5]–[8]. However, fabrication of such filters require complex multistage lithography and also it is incredibly challenging to make nanometer-thick filters which are more suited for flat silicon photonics platform for telecommunication applications, integrating with image sensors and making compact filters for biosensors. Since the observation by Ebbesen *et al.* [9] of enhanced optical transmission (EOT) through sub-wavelength holes in metal films, there has been a significant body

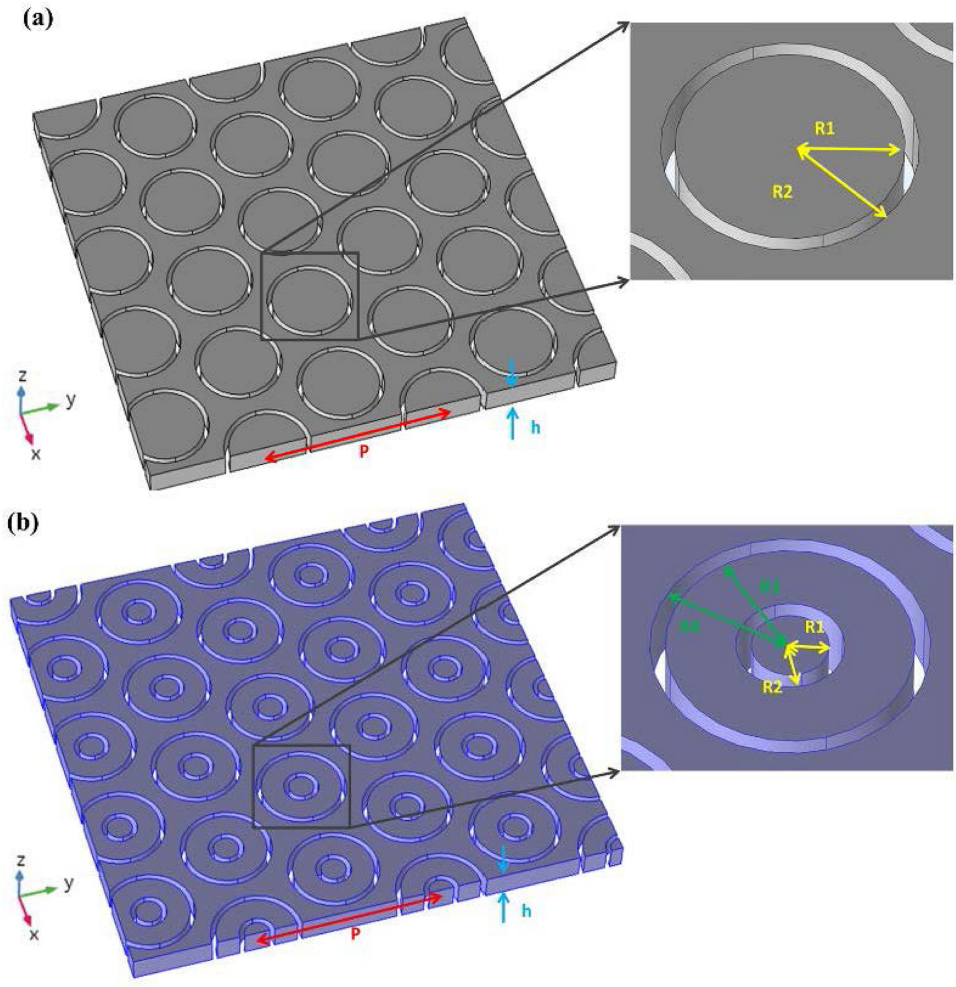

Fig. 1. (a) The schematic diagram of angular aperture array (AAA) in a hexagonal arrangement in the Silver film. The zoom-in inset shows the parameters used to design AAA; R_1 and R_2 refer to the inner and outer radii of the aperture. (b) The schematic diagram of double coaxial aperture array (DAA) in hexagonal arrangement in the Silver film. The zoom-in inset shows the parameters used to design DAA; R_1 and $_2$ refer to the inner and outer radii of the inner aperture, and R_3 and R_4 for the outer aperture, D refers to the distance between the two apertures ($D = R_3 - R_4$) and P, the pitch of DAA. The superstrate and substrate are not shown in the diagram for the unobstructed view.

of research into developing novel plasmonic spectral filters of various kinds [10]–[15]. A significant advantage of plasmonic filters is their tunability across a wide wavelength range using metal film with a thickness of the order of tens of nanometers [16]–[19]. Furthermore, they exhibit reduced crosstalk, are durable at high temperature, require a reduced set of materials and are resilient to prolonged exposure to ultraviolet radiation [20].

Roberts and McPhedran initially proposed bandpass filters consisting of arrays of annular apertures in a perfectly electrically conducting film with a view to potential applications in the far-infrared and visible regions of the spectrum [21]. Baida and Van Labeke [22], [23] subsequently investigated annular aperture arrays (AAA) which exhibit high transmission, with resonances in the visible or near-infrared regions of the electromagnetic spectrum. The research presented below is builds on our earlier computational investigations of AAAs for use in the millimeter wave and far-infrared regions of the electromagnetic spectrum [21], [24]–[28]. AAAs are promising candidates for developing spectral filters due to their tunability across the entire visible spectrum using a single nanometer thick metal film [9], [16], [17]. Fig. 1(a) shows one AAA, which exhibits transmission peaks resulting

from Fabry-Perot resonance supported by a cylindrical resonance cavity, which are formed by a metal film with finite thickness and two end faces. This aspect has been investigated numerically and experimentally demonstrated [24], [27], [29]–[33]. The main advantage of the AAA based filter is that the same resonance peak can be obtained through different combinations of the inner (R_1) and outer radius (R_2) (the average radius determines the resonance frequency but narrowing the gap, i.e., $g = R_2 - R_1$, also leads to red-shifting of the resonance) and transmission up to 90% has been demonstrated in the visible spectrum [33]. It has been reported that the location of maxima in the transmission spectrum can be estimated by solving the equation: $l = (n\pi - \Omega)/\beta$ [17], where l is the thickness of the metal film, n is the order of the Fabry-Pérot resonance, Ω is the phase of the reflection coefficient, and β is the propagation constant. Furthermore, AAA based plasmonic filters are superior to circular hole array-based filters because the location of the resonance peak in the transmission spectrum is relatively independent of the angle of incidence. This will ensure that the wavelengths filtered are the same irrespective of the incident angle or viewing angle. However, the resonance frequency of the AAA filter is difficult to tune in the near infrared region (NIR) due to the requirement for an extremely narrow gap (g) between the radii ($g = R_2 - R_1$). This is due to the red shift in the peak wavelength position of transmission spectrum requires a decrease in the gap in AAA. This requirement for decreasing gap with increasing wavelength makes fabrication of these structures very difficult in the NIR region. Recently, a double coaxial ring geometry and a double overlapped annular apertures demonstrated as a better candidate due to their plasmon resonances throughout the visible and the near-infrared spectral ranges and suitability to simulate wave guiding effects in nanotubes [26], [34]–[38].

In this paper, we present a double coaxial aperture array (DAA) in a hexagonal arrangement where fine-tuning of the resonance in the NIR region is achieved using two coaxial annular apertures. Fig. 1(a) shows the schematics of angular aperture array (AAA) and single angular aperture, where there are two relevant radii values, the inner (R_1) and outer (R_2) radii. For a double coaxial aperture, there are four relevant radii values, the inner (R_1) and outer (R_2) radii of the first coaxial aperture (gap1: $R_2 - R_1$) and the inner (R_3) and outer (R_4) radii of the second coaxial aperture (gap2: $R_4 - R_3$). Fig. 1(b) shows a double coaxial aperture array (DAA) and one double coaxial aperture (DA). Here, the gap between the radii (gap 1 and gap 2) can be kept constant and the spectral location of the transmission maximum can be tuned to any wavelength in the NIR region by varying only the radial distance ($D = R_3 - R_2$) between the two concentric coaxial apertures, i.e., D is varied by adjusting only the size of the inner apperture for tuning the peak wavelength position. The DAA has more degrees of freedom in its design parameters since four radii can be adjusted independently. When the gap between the inner and outer coaxial apertures in the DAA decreases, there is coupling between the localised plasmons in the two coaxial apertures [39]–[41]. This coupling increases the transmission in addition to a red-shift in the wavelength. This red-shift is used for the wavelength tuning. Using the DAA, an effective tuning of plasmon resonances in the near-infrared spectrum with high transmission is numerically demonstrated, followed by the demonstration of the angle-robust feature of DAA. The device presented here opens up the possibility of new plasmonic wavelength filters in the NIR region, particularly in the telecommunication wavelengths (i.e., O, E, S and C bands) for developing modulators, multi-spectral camera sensors and plasmonic biosensor devices.

2. Device Description and Simulation Results

We begin by showing simulations showing the performance of the DAA in a hexagonal arrangement. A hexagonal arrangement is preferable to a square arrangement due to its higher fill factor [38]. The DAA is computationally investigated using finite element methods (FEM) implemented in COMSOL MULTIPHYSICS 5.2. The schematic diagram of the DAA model is shown in Fig. 1. The simulation model to find the peak wavelength of the filters consists of a 100 nm silver (Ag) layer on a semi-infinite glass substrate with the refractive index of 1.5 and the region above and within they apertures is assumed to be a vacuum. To simulate an infinite periodic array, the unit cell consisted of a single aperture at the centre surrounded by one quadrant of each of the four neighbouring apertures and

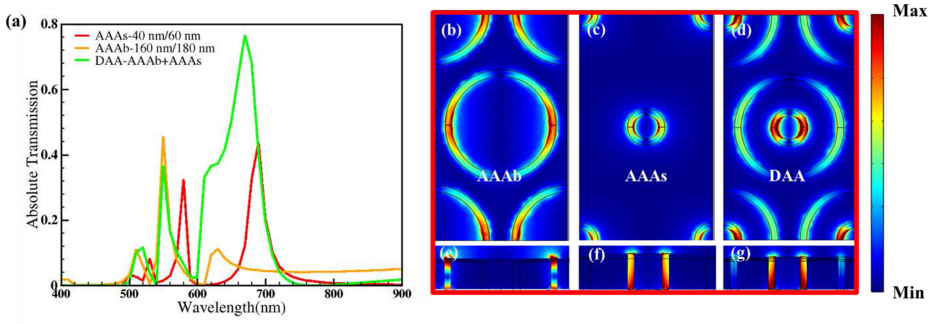

Fig. 2. Transmission spectra and formation of DAA from two AAA: (a) the simulated absolute transmission of AAAs, AAAb and DAA using the finite element method (FEM) over 400 nm to 900 nm wavelength range with peak resonances at 690 nm, 550 nm and 670 nm respectively. (b) and (e) show normalised electric field distribution (top view and cross-section view) for AAAb with a pitch of 430 nm at 550 nm peak wavelength. (c) and (f) show normalised electric field distribution (top view and cross-section view) for AAAs with a pitch of 430 nm at 690 nm peak wavelength. (d) and (g) show normalised electric field distribution (top view and cross-section view) for DAA which is the combination of AAAb and AAAs (AAAb + AAAs = DAA) at 670 nm peak wavelength. The cross-section view of the electric field shows characteristic of TE11 mode in each of the holes. The colour legend, the cold tone (blue) to warm tone (red) colour refers to minimum intensity to maximum intensity ($|E|^2$).

Table 1
Radii Values Used and Obtained Resonance Peaks in Fig. 2

Device	R1 nm	R2 nm	R3 nm	R4 nm	λ_{RES} nm
AAAb	160	180	NA	NA	550
AAAs	40	60	NA	NA	690
DAA	40	60	160	180	670

periodic boundary conditions applied on four sides. Both input and output are set as Periodic port with perfect match layer (PML) applied on top and bottom. The excitation was a plane wave incident from the Ag side where TE polarization is used throughout the paper. Port boundary conditions were used, and the transmission normalized to the incident power. For the consistency of simulation, the pitch size (P) is kept at 430 nm throughout the paper. The refractive indices of Ag for different wavelengths were taken from Johnston and Christy [42] and the refractive indices for quartz is taken as 1.5 at all wavelength.

Fig. 2 shows a DAA is designed by combining two AAA geometries, AAA large (AAAb) and AAA small (AAAs) along with the transmission spectra and electric field distribution on the apertures. The peak wavelength positions of the interest for AAAb and AAAs can be estimated by varing the radii values using COMSOL MULTIPHYSICS followed by combining them to obtain DAA. The transmission spectra are numerically obtained from 400 nm to 900 nm wavelength range for AAAs and AAAb with major peak resonances at 690 nm and 550 nm respectively. Then both AAAb and AAAs are combined with a distance between them to obtain a DAA to produce a peak resonance at 670 nm. Figs. 2(b)–(d) show the normalized electric field distribution in xy-plane for both top view and cross-section view for AAAb, AAAs and DAA at the above resonance peak positions, while Figs. (e)– (g) show cross-sections of electric field in holes in zx-plane (apertures) of AAAb, AAAs and DAA. The transverse electric field distribution exhibits the characteristic transverse profile of the TE_{11} mode in each of the holes. All radius values used for obtaining the spectra and fields of Fig. 2 are listed in Table 1. The distance between the coaxial apertures (D) is varied here by adjusting only the size of inner aperture for tuning the peak wavelength position.

Fig. 3 shows the transmission spectra obtained through DAA using the same gaps (g1 = g2 = 20 nm), keeping the dimensions of the outer ring (R3 − 160 nm and R4 − 180 nm) and the pitch 430 nm fixed, but varying the size of the inner ring (DAA1 − DAA10).The thickness of the Ag film used was kept fixed at 100 nm. In a DAA, preliminary resonance tuning can be performed using an

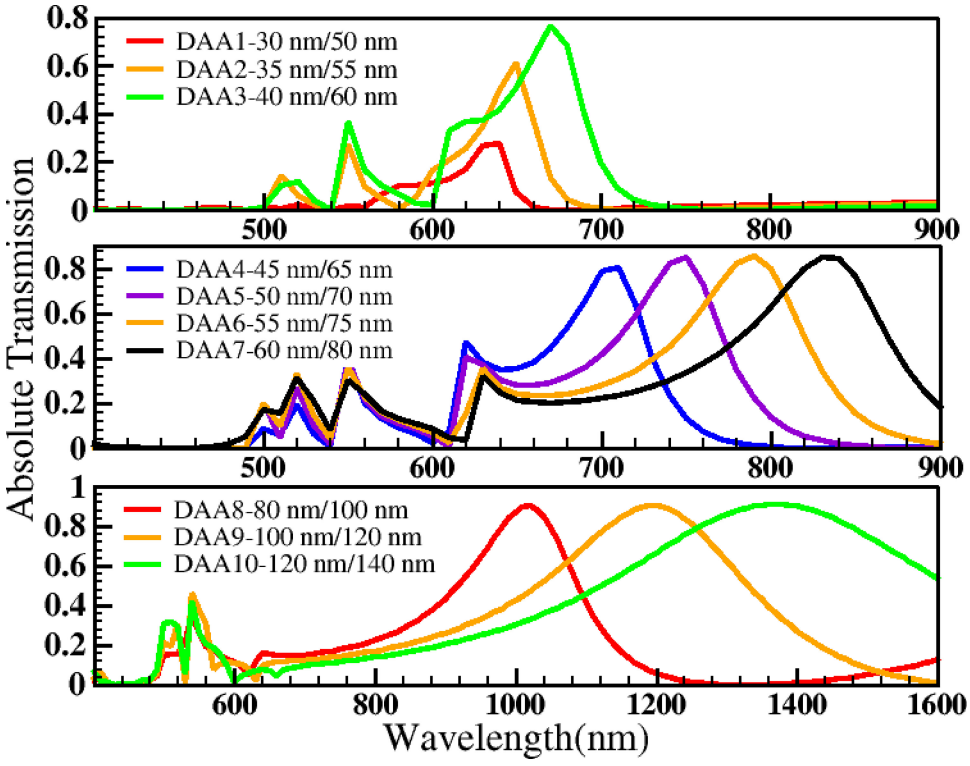

Fig. 3. Tuning of the resonance peak in a double coaxial aperture array (DAA) in a hexagonal arrangement. The simulation results are divided into three groups within the near infrared (NIR) region for easy review. By keeping the inner and outer radii of the outer coaxial hole constant (R_3 −160 nm and R_4 − 180 nm), the inner and outer radii of the inner coaxial hole was increased initially by a step of 5 nm starting from 30 nm (R_1) and 50 nm (R_2) (DAA1) to 60 nm (R_1) and 80 nm (R_2) (DAA7) and another step of 20 nm starting from 80 nm (R_1) and 100 nm (R_2) (DAA8) to 120 nm (R_1) and 140 nm (R_2) (DAA10). Table 2 shows the device parameters in detail along with the peak wavelengths in the NIR.

Table 2
Radii Values Used and Obtained Resonance Peaks in Fig. 4

Device	R_1	R_2	∗D (nm)	R_3	R_4	λ_{RES}	Spectral width FWHM (nm)
	Gap (nm), ∗g1=R2-R1			Gap (nm), g2=R4-R3			
DAA1	30	50	110	160	180	630	45
DAA2	35	55	105	160	180	650	45
DAA3	40	60	100	160	180	670	65
DAA4	45	65	95	160	180	710	65
DAA5	50	70	90	160	180	750	75
DAA6	55	75	85	160	180	790	90
DAA7	60	80	80	160	180	830	95
DAA8	80	100	60	160	180	1020	180
DAA9	100	120	40	160	180	1200	330
DAA10	120	140	20	160	180	1380	540

∗ g1 = g2 = 20 nm.
∗ D = distance between two concentric coaxial apertures.

AAA with only the outer coaxial aperture with a gap (g2). The second inner coaxial aperture can then be introduced by keeping the gap, g1 same as the g2. Table 2 shows optimized radius values for DAA geometries (DAA1 − DAA10) together with the corresponding resonance wavelengths (λ_{RES}). It is clear from the results shown in Fig. 4 that the tunability of demonstrated structure covers the wavelengths in the near infrared region (NIR) by merely varying size of the ring. Furthermore, it is

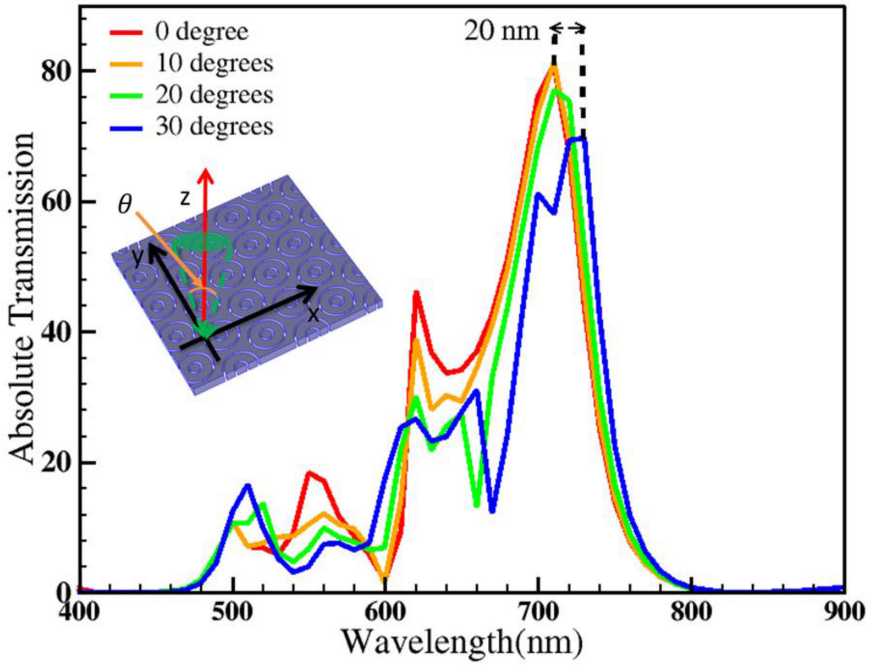

Fig. 4. Transmission spectrum of DAA for a different angle of incidences, θ (0 degrees, 10 degrees, 20 degrees, and 30 degrees). DAA4 was used for the study as given in the Table 2. DAA shows only minor peak shift concerning with angle incidence and variation of transmission percentage is negligible. Here the angle of incidence refers to the full field of view (θ), as shown in the inset.

observed that as the inner coaxial hole approaches the outer coaxial hole in the DAA, there is a red-shift in the wavelength and an enhancement in the transmission percentage as shown in Fig. 4. The availability of four degrees of freedom permits greater control of resonance in the near-infrared frequencies which enables to the realisation of new ultra-compact devices with sensitive response via a simple geometry control.

The DAA structure is further studied to find its sensitivity to angle of incidence. The results show that DAA can be designed to be insensitive to incident angle compared to the simple nano-hole array structure, due to the localized cylindrical surface plasmons supported in the coaxial holes. However, SPP modes can be supported in the coaxial hole array due to continuous metal film into which the DAA array is perforated. This can produce additional spectral features in the transmission spectrum and can also introduce an angular sensitivity. Due to the availability of four radii values, DAA geometry is possible to minimise this effect. Further simulations were carried out to study the angle dependence of DAA structure (DAA4 was used for the simulation). As shown in Fig. 4, for DAA4 the peak wavelength redshifts about 10 nm accompanied with a transmission reduction of approximately 10% at 30 degrees of incidence. These results are within the acceptable limit of angle insensitivity applications like [38]. These features are important in the design of modulators for telecommunications, plasmonic colour filters, plasmonic band pass filters, solar cells and sensors operating in the NIR region.

3. Conclusions

In conclusion, we have presented a double coaxial aperture array (DAA) in a hexagonal geometry where fine tuning of the resonance is achieved using two coaxial annular apertures in the NIR region. DAA has four radius values, the inner radius (R_1) and outer radius (R_2) of the first coaxial aperture with a gap ($g1 = R_2 - R_1$) and the inner radius (R_3) and outer radius (R_4) for the second aperture with a gap ($g2 = R_4 - R_3$). The gaps g1 and g2 can be kept constant for tuning peak

resonances (peak wavelengths) by varying distance between the two coaxial apertures. In contrast with AAA, this technique allows tuning of resonances to higher wavelengths without reducing the gap which makes the device fabrication and fine tuning less cumbersome. Furthermore, DAA has more degrees of freedom for tuning of the plasmonic resonances. Fine tuning of peak wavelengths with high transmission in the NIR and telecommunication bands are demonstrated along with its insensitivity to the angle of incidence. The DAAs find applications in plasmonic wavelength filters operating in the NIR region, filters for telecommunication wavelengths (O, E, S and C bands), multi-spectral image sensors and biosensors.

Acknowledgment

The numerical simulations were undertaken in the NCI National Facility in Canberra, Australia, which is supported by the Australian Commonwealth Government.

References

[1] R. Rajasekharan, T. D. Wilkinson, P. J. Hands, and Q. Dai, "Nanophotonic three-dimensional microscope," *Nano Lett.*, vol. 11, no. 7, pp. 2770–2773, 2011.
[2] Q. Dai *et al.*, "Transparent liquid-crystal-based microlens array using vertically aligned carbon nanofiber electrodes on quartz substrates," *Nanotechnology*, vol. 22, no. 11, 2011, Art. no. 115201.
[3] M. Vaughan, *The Fabry-Perot Interferometer: History, Theory, Practice and Applications*. Evanston, IL, USA: Routledge, 2017.
[4] S. Abbas, L. Dupont, I. Dozov, P. Davidson, and C. Chanéac, "Optical filter based on Fabry-Perot structure using a suspension of goethite nanoparticles as electro-optic material," *Proc. SPIE*, vol. 10555, 2018, Art. no. 105550G.
[5] B. Monacelli, J. B. Pryor, B. A. Munk, D. Kotter, and G. D. Boreman, "Infrared frequency selective surface based on circuit-analog square loop design," *IEEE Trans. Antennas Propag.*, vol. 53, no. 2, pp. 745–752, Feb. 2005.
[6] P. Kong, X.-W. Yu, M. Zhao, Y. He, L. Miao, and J. Jiang, "Switchable frequency selective surfaces absorber/reflector for wideband applications," *J. Electromagn. Waves Appl.*, vol. 29, no. 11, pp. 1473–1485, 2015.
[7] B. A. Munk, *Frequency Selective Surfaces: Theory and Design*. Hoboken, NJ, USA: Wiley, 2005.
[8] K. Sarabandi and N. Behdad, "A frequency selective surface with miniaturized elements," *IEEE Trans. Antennas Propag.*, vol. 55, no. 5, pp. 1239–1245, May 2007.
[9] T. W. Ebbesen, H. J. Lezec, H. F. Ghaemi, T. Thio, and P. A. Wolff, "Extraordinary optical transmission through sub-wavelength hole arrays," *Nature*, vol. 391, no. 6668, pp. 667–669, 1998. [Online]. Available: http://dx.doi.org/10.1038/35570
[10] C. Yang *et al.*, "Angle robust reflection/transmission plasmonic filters using ultrathin metal patch array," *Adv. Opt. Mater.*, vol. 4, no. 12, pp. 1981–1986, 2016.
[11] Z. Li, A. W. Clark, and J. M. Cooper, "Dual color plasmonic pixels create a polarization controlled nano color palette," *ACS Nano*, vol. 10, no. 1, pp. 492–498, 2016.
[12] C. Genet and T. Ebbesen, "Light in tiny holes," *Nature*, vol. 445, no. 7123, pp. 39–46, 2007.
[13] Z.-L. Deng *et al.*, "Diatomic metasurface for vectorial holography," *Nano Lett.*, vol. 18, no. 5, pp. 2885–2892, 2018.
[14] Z.-L. Deng and G. Li, "Metasurface optical holography," *Mater. Today Phys.*, vol. 3, pp. 16–32, 2017.
[15] Z. Deng, Y. Cao, X. Li, and G. Wang, "Multifunctional metasurface: From extraordinary optical transmission to extraordinary optical diffraction in a single structure," *Photon. Res.*, vol. 6, no. 5, pp. 443–450, 2018.
[16] S. G. Rodrigo, F. de León-Pérez, and L. Martín-Moreno, "Extraordinary optical transmission: Fundamentals and applications," *Proc. IEEE*, vol. 104, no. 12, pp. 2288–2306, Dec. 2016. [Online]. Available: https://ieeexplore.ieee.org/document/7592449/
[17] M. Haftel, C. Schlockermann, and G. Blumberg, "Role of cylindrical surface plasmons in enhanced transmission," *Appl. Phys. Lett.*, vol. 88, 2006, Art. no. 193104. [Online]. Available: https://doi.org/10.1063/1.2201884
[18] M. Sun *et al.*, "A photonic switch based on a hybrid combination of metallic nanoholes and phase-change vanadium dioxide," *Sci. Rep.*, vol. 8, 2018, Art. no. 11106.
[19] S. Wang *et al.*, "Angular momentum-dependent transmission of circularly polarized vortex beams through a plasmonic coaxial nanoring," *IEEE Photon. J.*, vol. 10, no. 1, Feb. 2018, Art. no. 5700109.
[20] S. Yokogawa, S. P. Burgos, and H. A. Atwater, "Plasmonic color filters for CMOS image sensor applications," *Nano Lett.*, vol. 12, no. 8, pp. 4349–4354, 2012. [Online]. Available: https://pubs.acs.org/doi/10.1021/nl302110z
[21] A. Roberts and R. C. McPhedran, "Bandpass grids with annular apertures," *IEEE Trans. Antennas Propag.*, vol. 36, no. 5, pp. 607–611, May 1988. [Online]. Available: https://ieeexplore.ieee.org/document/192136/
[22] F. Baida and D. Van Labeke, "Light transmission by subwavelength annular aperture arrays in metallic films," *Opt. Commun.*, vol. 209, no. 1–3, pp. 17–22, 2002. [Online]. Available: https://www.sciencedirect.com/science/article/abs/pii/S0030401802016905
[23] F. Baida, Y. Poujet, B. Guizal, and D. Van Labeke, "New design for enhanced transmission and polarization control through near-field optical microscopy probes," *Opt. Commun.*, vol. 256, no. 1–3, pp. 190–195, 2005. [Online]. Available: https://www.sciencedirect.com/science/article/abs/pii/S0030401805006760
[24] A. Roberts, "Beam transmission through hole arrays," *Opt. Exp.*, vol. 18, no. 3, pp. 2528–2533, 2010. [Online]. Available: https://www.osapublishing.org/oe/abstract.cfm?uri=oe-18-3-2528

[25] R. Rajasekharan Unnithan *et al.*, "Plasmonic colour filters based on coaxial holes in aluminium," *Materials*, vol. 10, no. 4, 2017. [Online]. Available: http://www.mdpi.com/1996-1944/10/4/383
[26] R. Rajasekharan and A. Roberts, "Optical 'magnetic mirror' metasurfaces using interference between fabry-pérot cavity resonances in coaxial apertures," *Sci. Rep.*, vol. 5, 2015, Art. no. 10297. [Online]. Available: http://dx.doi.org/10.1038/srep10297
[27] S. Orbons and A. Roberts, "Resonance and extraordinary transmission in annular aperture arrays," *Opt. Exp.*, vol. 14, no. 26, pp. 12623–12628, 2006. [Online]. Available: https://www.osapublishing.org/oe/abstract.cfm?uri=oe-14-26-12623
[28] P. A. Krug, D. H. Dawes, R. C. McPhedran, W. Wright, J. C. Macfarlane, and L. B. Whitbourn, "Annular-slot arrays as far-infrared bandpass filters," *Opt. Lett.*, vol. 14, no. 17, pp. 931–933, 1989. [Online]. Available: http://ol.osa.org/abstract.cfm?URI=ol-14-17-931
[29] B. Heshmat, D. Li, T. E. Darcie, and R. Gordon, "Tuning plasmonic resonances of an annular aperture in metal plate," *Opt. Exp.*, vol. 19, no. 7, pp. 5912–5923, 2011. [Online]. Available: https://www.osapublishing.org/oe/abstract.cfm?uri=oe-19-7-5912
[30] M. I. Haftel, C. Schlockermann, and G. Blumberg, "Enhanced transmission with coaxial nanoapertures: Role of cylindrical surface plasmons," *Phys. Rev. B*, vol. 74, no. 23, 2006, Art. no. 235405.
[31] J. Salvi *et al.*, "Annular aperture arrays: Study in the visible region of the electromagnetic spectrum," *Opt. Lett.*, vol. 30, no. 13, pp. 1611–1613, 2005. [Online]. Available: https://www.osapublishing.org/ol/abstract.cfm?uri=ol-30-13-1611
[32] G. Si *et al.*, "Annular aperture array based color filter," *Appl. Phys. Lett.*, vol. 99, no. 3, 2011, Art. no. 033105. [Online]. Available: https://aip.scitation.org/doi/10.1063/1.3608147
[33] Y. Poujet, J. Salvi, and F. I. Baida, "90 in the visible range through annular aperture metallic arrays," *Opt. Lett.*, vol. 32, no. 20, pp. 2942–2944, 2007. [Online]. Available: https://www.osapublishing.org/ol/abstract.cfm?uri=ol-32-20-2942
[34] H. Xu, H. Li, and G. Xiao, "Tunable plasmon resonance coupling in coaxial gold nanotube arrays," *Chin. Opt. Lett.*, vol. 11, no. 4, 2013, Art. no. 042401.
[35] X. Jiang *et al.*, "Controlling light through double-ring arrays," in *Proc. IEEE Photon. Global Conf.*, 2012, pp. 1–4.
[36] H. Liu, N. Wang, Y. Liu, Y. Zhao, and X. Wu, "Light transmission properties of double-overlapped annular apertures," *Opt. Lett.*, vol. 36, no. 3, pp. 385–387, 2011. [Online]. Available: http://ol.osa.org/abstract.cfm?URI=ol-36-3-385
[37] F. Hao, P. Nordlander, M. T. Burnett, and S. A. Maier, "Enhanced tunability and linewidth sharpening of plasmon resonances in hybridized metallic ring/disk nanocavities," *Phys. Rev. B*, vol. 76, no. 24, 2007, Art. no. 245417.
[38] R. Rajasekharan *et al.*, "Filling schemes at submicron scale: Development of submicron sized plasmonic colour filters," *Sci. Rep.*, vol. 4, 2014, Art. no. 6435.
[39] N. Mou *et al.*, "Hybridization-induced broadband terahertz wave absorption with graphene metasurfaces," *Opt. Exp.*, vol. 26, no. 9, pp. 11 728–11 736, 2018.
[40] Z. Fang *et al.*, "Gated tunability and hybridization of localized plasmons in nanostructured graphene," *ACS Nano*, vol. 7, no. 3, pp. 2388–2395, 2013.
[41] E. Prodan, C. Radloff, N. J. Halas, and P. Nordlander, "A hybridization model for the plasmon response of complex nanostructures," *Science*, vol. 302, no. 5644, pp. 419–422, 2003.
[42] P. B. Johnson and R.-W. Christy, "Optical constants of the noble metals," *Phys. Rev. B*, vol. 6, no. 12, 1972, Art. no. 4370.